

“Simulating Synthesis”: Ceria Nanosphere Self-Assembly into Nanorods and Framework Architectures

Dean C. Sayle,^{*,†} Xiangdong Feng,^{*,‡,||} Yong Ding,[§] Zhong Lin Wang,^{*,§} and Thi X. T. Sayle[†]

Contribution from the Department of Materials and Applied Science, Defence College of Management and Technology, Cranfield University, Defence Academy of the United Kingdom, Shrivenham, Swindon SN6 8LA, U.K., College of Chemistry and Chemical Engineering, Hunan Normal University, Changsha, Hunan, P. R. China, and School of Materials Science and Engineering, Georgia Institute of Technology, Atlanta, GA30332-0245, USA

Received February 21, 2007; E-mail: d.c.sayle@cranfield.ac.uk; shawn.feng@Jhresearchusa.com; zhong.wang@mse.gatech.edu

Abstract: We predict, from computer modeling and simulation in partnership with experiment, a general strategy for synthesizing spherical oxide nanocrystals via crystallization from melt. In particular we “simulate synthesis” to generate full atomistic models of undoped and Ti-doped CeO₂ nanoparticles, nanorods, and nanoporous framework architectures. Our simulations demonstrate, in quantitative agreement with experiment [*Science* **2006**, 312, 1504], that Ti (dopant) ions change the shape of CeO₂ nanocrystals from polyhedral to spherical. We rationalize this morphological change by elucidating, at the atomistic level, the mechanism underpinning its synthesis. In particular, CeO₂ nanocrystals can be synthesized via crystallization from melt: as a molten (undoped) CeO₂ nanoparticle is cooled, nucleating seeds spontaneously evolve at the *surface* and express energetically stable {111} facets to minimize the energy. As crystallization proceeds, the {111} facets grow, thus facilitating a polyhedral shape. Conversely, when doped with Ti, a (predominantly) TiO₂ shell encapsulates the inner CeO₂ core. This shell inhibits the evolution of nucleating seeds at the surface thus rendering it amorphous during cooling. Accordingly, crystallization is forced to proceed via the evolution of a nucleating seed in the *bulk* CeO₂ region of the nanoparticle, and as this seed grows, it remains surrounded by amorphous ions, which “wrap” around the core so that the energies for high-index facets are drastically reduced; these amorphous ions adopt a spherical shape to minimize the surface energy. Crystallization emanates radially from the nucleating seed, and because it is encapsulated by an amorphous shell, the crystallization front is not compelled to express energetically favorable surfaces. Accordingly, after the nanoparticle has crystallized it retains this spherical shape. A typical animation showing the crystallization (with atomistic detail) is available as Supporting Information. From this data we predict that spherical oxide nanocrystals can be synthesized via crystallization from melt in general by suppressing nucleating seed evolution at the surface thus forcing the nucleating seed to spontaneously evolve in the bulk. Nanospheres can, similar to zeolitic classifications, constitute Secondary Building Units (SBUs) and can aggregate to form nanorods and nanoporous framework architectures. Here we have attempted to simulate this process to generate models for CeO₂ and Ti-doped CeO₂ nanorods and framework architectures. In particular, we predict that Ti doping will “smooth” the surfaces: hexagonal prism shaped CeO₂ nanorods with {111} and {100} surfaces become cylindrical, and framework architectures change from faceted pores and channels with well-defined {111} and {100} surfaces to “smooth” pores and channels (expressing both concave and convex curvatures). Such structures are difficult to characterize using, for example, Miller indices; rather we suggest that these new structural materials may be better described using minimal surfaces.

Introduction

The revolution that is “nanoscience” has led to unprecedented research efforts focused on synthesizing nanomaterials with controllable shapes, sizes, and assemblages, with the promise of new and tuneable properties spanning a range of applications.¹

An illustration of the diversity of nanomaterials can be seen in Figure 1. The stark contrast between cubic, Figure 1a,b, and spherical, Figure 1c, CeO₂ nanocrystals demonstrates clearly the ability to actively design and engineer nanostructures to facilitate a particular desirable attribute or property. In particular, cubic nanocrystals proffer tailored catalytic properties; the {100} surface exposed at each face of the cube is highly reactive, Figure 1a,b. Conversely, spherical nanocrystals, Figure 1c, are

[†] Defence Academy of the United Kingdom.

[‡] Hunan Normal University.

[§] Georgia Institute of Technology.

^{||} Current address: James Hardie Building Products, 10901, Elm Avenue, Fontana, California 92337, U.S.A.

(1) Zhang, H.; Edwards, E. W.; Wang, D. Y.; Mohwald, H. *Phys. Chem. Chem. Phys.* **2006**, 8, 3288–3299.

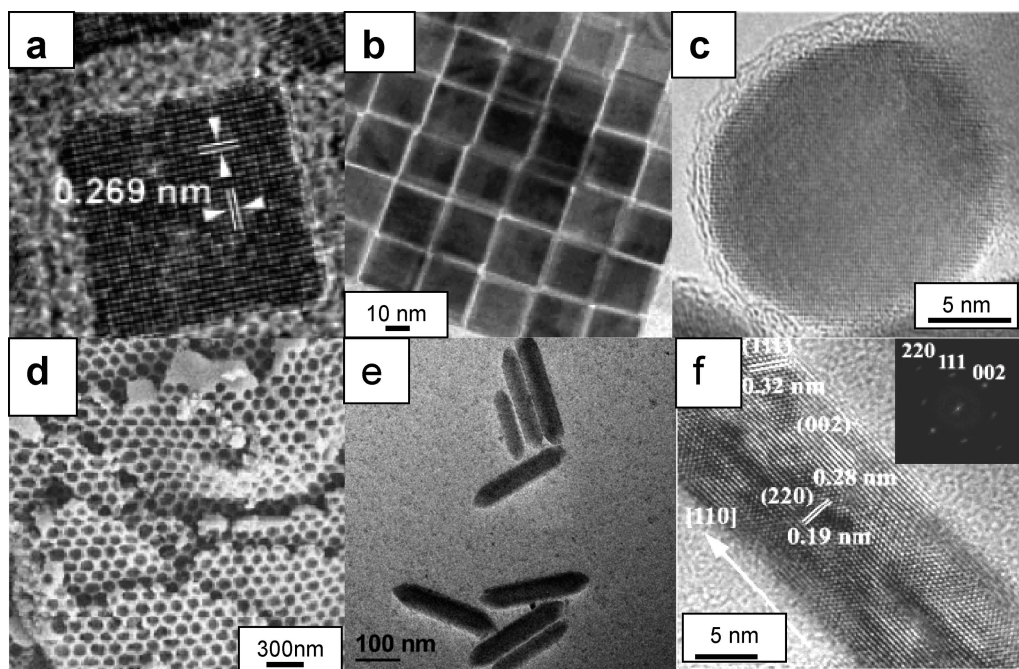


Figure 1. High-resolution electron micrographs of ceria, CeO₂: (a) Single cuboidal CeO₂ nanocrystal (all {100}) and (b) ordered array of nanocubes. [Reprinted with permission from ref 5. Copyright 2006 American Chemical Society.] (c) Single spherical Ti-doped CeO₂ nanocrystal. [Reprinted with permission from ref 2. Copyright 2006 the American Association for the Advancement of Science.] (d) Nanoporous CeO₂. [Reprinted with kind permission from ref 3. Copyright 2006 Springer Science and Business Media.] (e) Self-assembled CeO₂ nanoparticles into CeO₂ nanorods. [Reprinted with permission from ref 4. Copyright 2005 American Chemical Society.] (f) Segment of a CeO₂ nanorod. [Reprinted with permission from ref 6. Copyright 2005 American Chemical Society.]

ideal as nanoabrasives; the absence of corners or edges prevents these nanocrystals from gouging the surfaces of the materials they planarize. Instead they act like ball bearings and polish the surfaces without scratching. Nanoabrasives accounted for 60% of the \$1 billion market in nanomaterials in 2005.² Mesoporous CeO₂, Figure 1d, was synthesized by Wang and co-workers using a polymeric scaffold to facilitate framework architectures.³ Kuiry and co-workers⁴ were able to coax CeO₂ nanoparticles to self-assemble and form nanorods, Figure 1e; a single high-resolution transmission electron micrograph of a CeO₂ nanorod is shown in Figure 1f.

Structural characterization at the atomistic level of nanomaterials, such as those in Figure 1, is crucial for the quantification and prediction of their physical, chemical, and mechanical properties. However, as their complexity increases, so do the challenges involved in unravelling their structure. Molecular simulation and modeling have provided experiment with invaluable insights and predictions for over 30 years. However such simulations now face serious challenges. In particular, contemporary materials are becoming so complex that it may soon be impossible to generate models that are sufficiently realistic to describe them adequately. Structural complexity evolves during synthesis, and therefore one way of capturing such complexity within atomistic models is to "simulate synthesis". Here, we attempt such a strategy and generate full atomistic models of pure and titanium-doped ceria nanomaterials including nano-

spheres, nanorods, and framework architectures by simulating, in part, the synthetic method used to manufacture them.

"Simulating" Synthesis. CeO₂ nanoparticles, nanorods, and framework architectures have all been synthesized experimentally.^{2,4,7} In all cases the final structures are highly sensitive to the fine detail of the synthetic method and conditions, for example, the particular solvent or surfactant, pH gradients, environmental conditions of temperature and pressure, contaminants, time, etc. The combinations and permutations are inexhaustible. Nevertheless, science has explored these conditions in an attempt to map "synthetic phase space". Clearly, as evidenced from the beautiful and complex nanostructures such as those shown in Figure 1, the syntheticist has been able to introduce intelligent design into their synthetic strategies by building upon this considerable body of data, to facilitate desirable structures with tailored properties.

To simulate synthesis is a daunting prospect for the theoretician, yet this may prove to be the only way that simulation and modeling of the future can continue to be of predictive value to experiment. Certainly this idea is not new and has been realized by simulators for many years. Indeed, a considerable body of work is focused toward understanding particular aspects pertaining to synthesis by modeling and simulation. For example, Hamad et al. have provided detailed insights into the evolution of embryonic clusters that may lead to the formation of nucleating seeds.⁸ Piana and co-workers have simulated

(2) Feng, X. D.; Sayle, D. C.; Wang, Z. L.; Paras, M. S.; Santora, B.; Sutorik, A. C.; Sayle, T. X. T.; Yang, Y.; Ding, Y.; Wang, X. D.; Her, Y. S. *Science* **2006**, *312*, 1504–1508.
 (3) Wang, T. W.; Sel, O.; Djerdj, I.; Smarsly, B. *Colloid and Polymer Science* **2006**, *285*, 1–9.
 (4) Kuiry, S. C.; Patil, S. D.; Deshpande, S.; Seal, S. *J. Phys. Chem.* **2005**, *109*, 6936–6939.

(5) Yang, S. W.; Gao, L. *J. Am. Chem. Soc.* **2006**, *128*, 9330–9331.
 (6) Mai, H. X.; Sun, L. D.; Zhang, Y. W.; Si, R.; Feng, W.; Zhang, H. P.; Liu, H. C.; Yan, C. H. *J. Phys. Chem. B* **2005**, *109*, 24380–24385.
 (7) Deshpande, A. S.; Pinna, N.; Smarsly, B.; Antonietti, M.; Niederberger, M. *Small* **2005**, *1*, 313–316.
 (8) Hamad, S.; Cristol, S.; Catlow, C. R. A. *J. Am. Chem. Soc.* **2005**, *127*, 2580–2590.

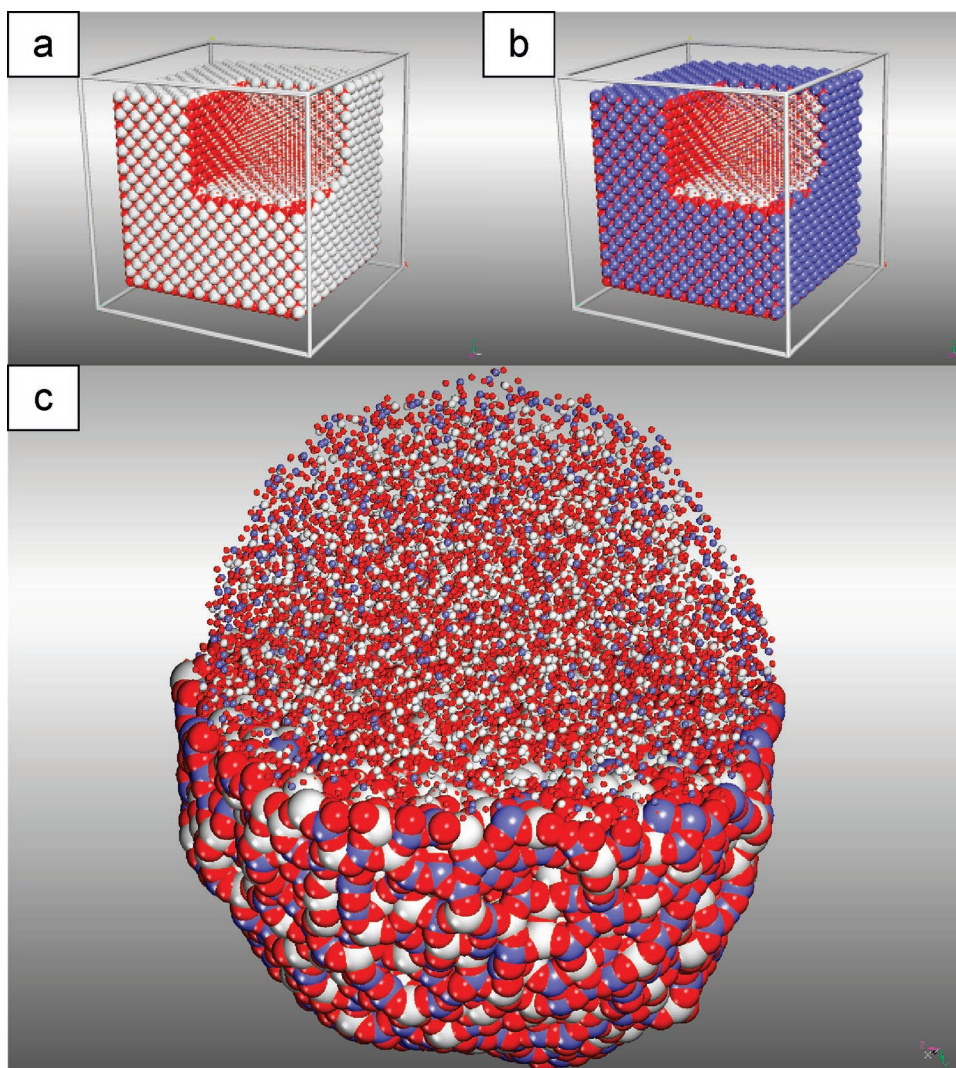


Figure 2. (a) CeO_2 starting structure; (b) Ti-doped CeO_2 ; (c) amorphous Ti– CeO_2 . Ce is white, Ti, blue, and O, red. The sphere sizes have been changed to allow viewing of the inner structure.

dissolution and crystallization at surfaces with dislocations to gauge how structural imperfections may influence structure and morphology.⁹ Sayle and co-workers have simulated atom deposition to form thin films.¹⁰ Even genetic algorithms, taking their cue from evolution itself, have been used to understand synthesis and structure.¹¹ Each of these simulations explores a particular window in synthetic phase space, in some cases, with meticulous attention to detail.

Here, we simulate synthesis as a means of introducing structural complexity into a complete and fully atomistic model. However, computational limitations entail that we must make severe approximations. These are necessary to marry computational cost with available facilities. On the other hand, in the future, one can build upon the results, generated here, to increase the similarity with experiment and thus facilitate more accurate models. However, first we must examine where the approximations should lie to ensure that they do not impinge, too severely, upon the results.

A simplistic “sketch” of the synthetic strategies for manufacturing nanoparticles, nanorods, and framework architectures that we have endeavored to follow may be described as follows: **Nanoparticles** - gas phase formation of amorphous/molten oxide nanoparticles in flame, which crystallizes upon cooling;² **nanorods** - spontaneous self-assembly of nanoparticles into nanorods;⁴ **framework architectures** - nanoparticles self-assemble to form amorphous nanoporous materials followed by crystallization in a vacuum.^{12,13,7}

Two key components that must be accommodated within the simulated synthesis include the following: First, the formation of amorphous nanoparticles and their self-assembly into nanorods and nanoporous architectures, which facilitates the general three-dimensional shape of the nanomaterial, and second, crystallization from the amorphous oxide precursors, which is necessary to introduce important microstructural features including morphology and surfaces exposed, accommodation of the lattice misfit between CeO_x and TiO_x , (misfit) dislocations,

(9) Piana, S.; Reyhani, M.; Gale, J. D. *Nature* **2005**, *438*, 70–73.
 (10) Sayle, D. C.; Maicaneanu, S. A.; Slater, B.; Catlow, C. R. A. *J. Mater. Chem.* **1999**, *9*, 2779–2787.
 (11) Sayle, D. C.; Johnston, R. L. *Curr. Opin. Solid State Mater. Sci.* **2003**, *7*, 3–12.

(12) Lu, D.; Katou, T.; Uchida, M.; Kondo, J. N.; Domen, K. *Chem. Mater.* **2005**, *17*, 632–637.
 (13) Chane-Ching, J. Y.; Cobo, F.; Aubert, D.; Harvey, H. G.; Airiau, M.; Corma, A. *Chem.—Eur. J.* **2005**, *11*, 979–987.

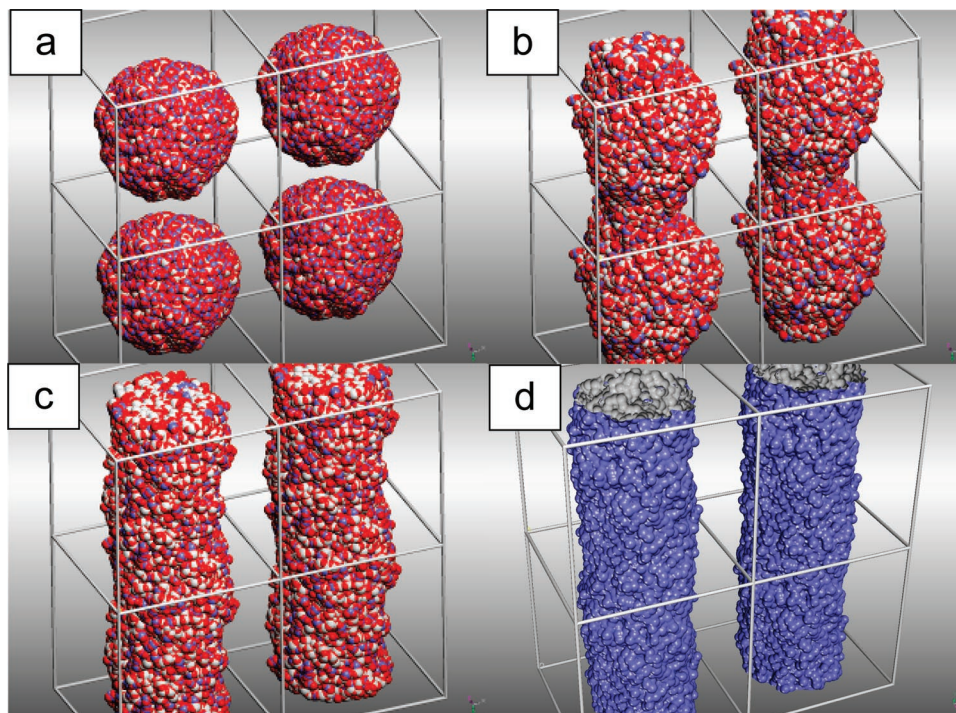


Figure 3. Strategy for generating ceria nanorods via the self-assembly of amorphous CeO₂ nanoparticles: (a) periodic array of (amorphous) Ti–CeO₂ nanoparticles (Figure 2c after 20 ps of MD simulation) in which the size of the simulation cell has been reduced to facilitate interaction between neighboring nanoparticles; (b) after 80 ps of MD simulation showing the evolution of the basic nanorod configuration; (c) after 1000 ps; (d) is analogous to (c) but with surface rendering to show more clearly the basic nanorod outline shape.

grain-boundaries and grain-junctions and intrinsic point defects, ionic relaxation.

Methods

Pure CeO₂ and Ti-doped CeO₂ were described using the Born model of the ionic solid, which includes long-range Coulombic terms coupled with short-range repulsive and rigid-ion interactions. Parameters have been published previously.^{14,15} The parameters have been used successfully many times before to model surfaces, thin films, defect energies, and ionic transport,^{16–18} and therefore we expect they will prove reliable for this present study. All the molecular dynamics (MD) simulations were performed using the DL_POLY code¹⁹ with three-dimensional periodic boundary conditions imposed throughout.

Generating Atomistic Models. Two identical “cubes” of CeO₂, comprising 15 972 atoms (5324 Ce, 10 648 O), were generated (Figure 2a,b). One cube was doped with 25 atom % Ti (1330 Ce⁴⁺ atoms, located at the surface, were replaced by Ti⁴⁺), while the other nanoparticle remained “pure”.

To facilitate nanocrystals, the size of the simulation cell was sufficiently large to prevent any interaction of the nanoparticle with its neighbors (images). Each nanoparticle was amorphized (tension induced following¹⁵) using MD simulation performed for 50 ps at 3750 K. The amorphous structures (amorphous Ti–CeO₂ is shown in Figure 2c) were then recrystallized by performing MD simulations at 3750 K

for 4000 ps and finally cooled to 273 K. Feng and co-workers have synthesized spherical nanoparticles of CeO₂ and Ce_{1–x}Ti_xO₂ (0 ≤ x ≤ 0.25).² We also simulated this range of Ti-doping. However, here we only report the 25% Ti-doped CeO₂ because it showed the most marked change compared with the undoped CeO₂ nanoparticle.

Nanorods were generated by reducing the size of the simulation “box”, Figure 2a,b, in one dimension. The nanoparticles were then melted by performing MD simulations at 8000 K for 1000 ps. The reduced simulation cell size facilitated interactions between neighboring (image) nanoparticles, and as the nanoparticles became molten, they aggregated together resulting, ultimately, in the formation of a nanorod, Figure 3. The CeO₂ and Ti–CeO₂ nanorods were then crystallized by performing MD simulation for 3827 ps at 3750 K and for 12 000 ps at 2500 K, respectively, and then cooled to 10 K. Ceria nanorods have been synthesized.^{4,6}

Our strategy for generating atomistic models was to crystallize them from amorphous precursors. However, similar to experiment, it is difficult to choose parameters that will facilitate a successful crystallization. For example, if the temperature is too high, the system will remain amorphous/molten. Conversely, if it is too low, the time for a nucleating seed to evolve followed by crystallization of the rest of the system is prohibitively long. For example, when we attempted to crystallize Ti-doped CeO₂ nanorods using the same temperature that was used to successfully crystallize the pure (undoped) CeO₂, it remained amorphous/molten and therefore we had to reduce the temperature accordingly to facilitate crystallization. In addition, the duration of the crystallization will change for different systems and temperatures. We found that reducing the temperature caused the speed of crystallization to slow. All the simulations performed in this study were run sufficiently long to ensure complete crystallization of each system.

Nanoporous framework architectures were generated by modifying the simulation cell to ensure that the nanoparticles interact with their neighbors (image) in all three dimensions. This procedure follows that

(14) Sayle, D. C.; Catlow, C. R. A.; Perrin, M. A.; Nortier, P. J. *Phys. Chem. Solids* **1995**, *56*, 799–805.

(15) Sayle, T. X. T.; Parker, S. C.; Sayle, D. C. *Chem. Commun.* **2004**, 2438–2439

(16) Sayle, T. X. T.; Parker, S. C.; Catlow, C. R. A. *Surf. Sci.* **1994**, *316*, 329–336.

(17) Sayle, T. X. T.; Parker, S. C.; Sayle, D. C. *J. Mater. Chem.* **2006**, *16*, 1067–1081.

(18) Balducci, G.; Islam, M. S.; Kaspar, J.; Fornasiero, P.; Graziani, M. *Chem. Mater.* **2000**, *12*, 677–681.

(19) Smith, W.; Forester, T. R. DL_POLY, copyright by the council for the Central Laboratory of the Research Councils, Daresbury Laboratory, Daresbury, Warrington, UK, 1996; www.cse.clrc.ac.uk/msi/software/DL_POLY/.

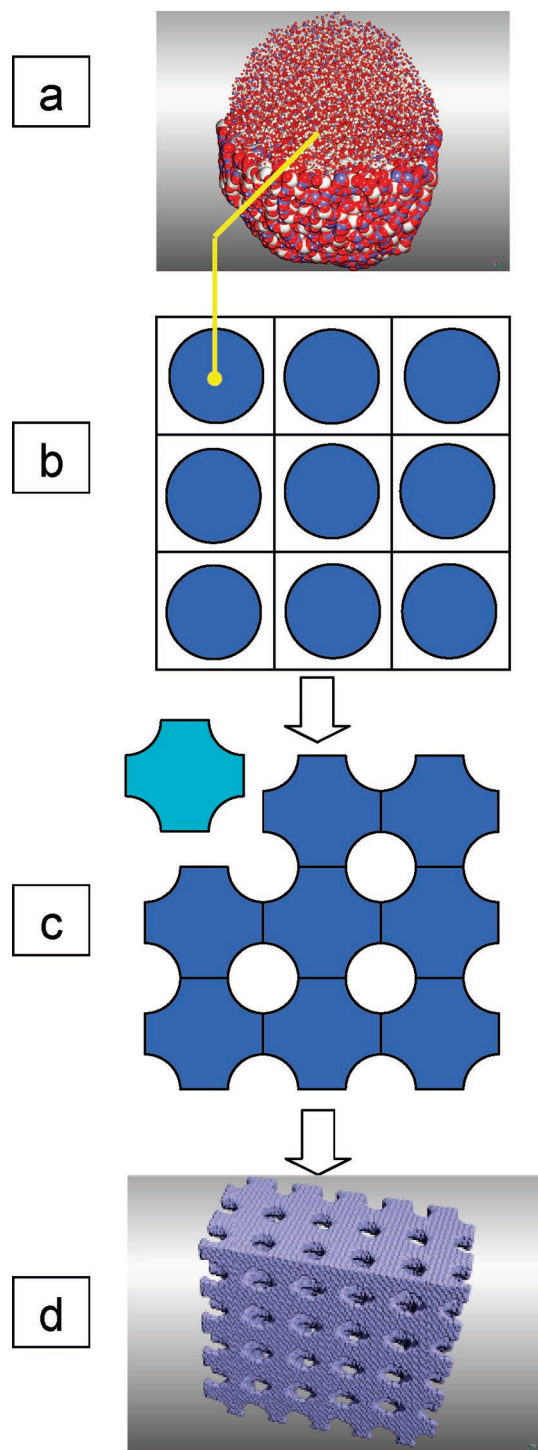


Figure 4. Self-assembly of amorphous Ti–CeO₂ nanospheres into nanoporous framework architectures. (a) Single amorphous Ti–CeO₂ nanosphere (as shown in Figure 1c); (b) periodic array of nanospheres within a simulation cell that is sufficiently small to facilitate aggregation of neighboring particles; (c) aggregated particles showing the channel system they facilitate; (d) framework model showing the connectivity of pores via a 3D channel system. (a) and (d) are fully atomistic models; (b) and (c) are schematics.

of our previous study on ZnS.²⁰ The nanoparticles were melted by performing MD simulation at 6000 K for 500 ps. Upon melting, the nanoparticles aggregated, facilitating the formation of three-dimensional framework architectures. The framework CeO₂ and Ti–CeO₂

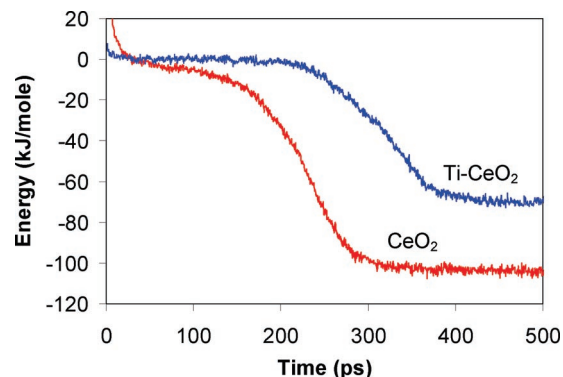


Figure 5. Configurational energy of CeO₂ (red) and Ti–CeO₂ (blue) nanoparticles, calculated as a function of time, during crystallization at 3750 K. The difference in energy between the first and second plateau reflects loosely the latent heat of crystallization. The energies of the first plateaus for CeO₂ and Ti–CeO₂ were normalized to zero.

architectures were then crystallized by performing MD simulation at 3750 K for 1660 ps and 2600 K for 5183 ps, respectively. The frameworks were then cooled to 10 K; schematics, describing this process, are shown in Figure 4. Synthetic strategies can be found in refs 7, 12, and 13.

Our simulations on the isolated nanocrystal are relatively close to experiment. However, the nanorods and nanoporous materials are generally facilitated using a “molecular scaffold”,^{3,1,21} Templating can be simulated,²² but this would prove prohibitively computationally expensive; rather we perform our simulations at constant volume, which acts, albeit rather artificially, as a scaffold. Conversely, we note that Lu and co-workers crystallized, successfully, Nb–Ta and Mg–Ta mixed oxides in a vacuum starting from amorphous precursors.¹²

Results

Simulated Crystallization. In this section we explore the crystallization and evolution into the final, low-temperature structures.

The configuration energy, calculated as a function of time, of the CeO₂ and Ti–CeO₂ nanocrystals is shown in Figure 5 and depicts graphically the crystallization. The configurational energies initially plateau (normalized to zero) and then drop gradually to plateau a second time. The energy difference between the first and second plateaus reflects the latent heat of crystallization. Both the CeO₂ and Ti–CeO₂ take about 200 ps to crystallize. However, the crystallization between the two is crucially different. In particular, the crystalline seed in Ti–CeO₂ evolves in (approximately) the *center* of the amorphous nanoparticle, Figure 6, enveloped by an amorphous sea of ions. Conversely, crystallization in pure CeO₂ is facilitated by a nucleating seed, which spontaneously evolves at the *surface*, Figure 7, and exposes the (most stable) CeO₂(111) surface. Both seeds conform to the fluorite crystal structure.

We also note that only one seed evolves in the Ti–CeO₂ resulting in the formation of a single (nano)crystal. In contrast, two crystalline seeds evolve, Figure 7b, in the undoped CeO₂ (both evolve at the surface), and as the crystallization fronts emanating from each seed consume the surrounding amorphous CeO₂, they impinge upon one another facilitating the formation of a general grain boundary, Figure 7c. A molecular graphics movie, showing the crystallization of the Ti–CeO₂ emanating

(21) Smarsly, B.; Antonietti, M. *Eur. J. Inorg. Chem.* **2006**, 6, 1111–1119
 (22) Lewis, D. W.; Willock, D. J.; Catlow, C. R. A.; Thomas, J. M.; Hutchings, G. J. *Nature* **1996**, 382, 604–606.

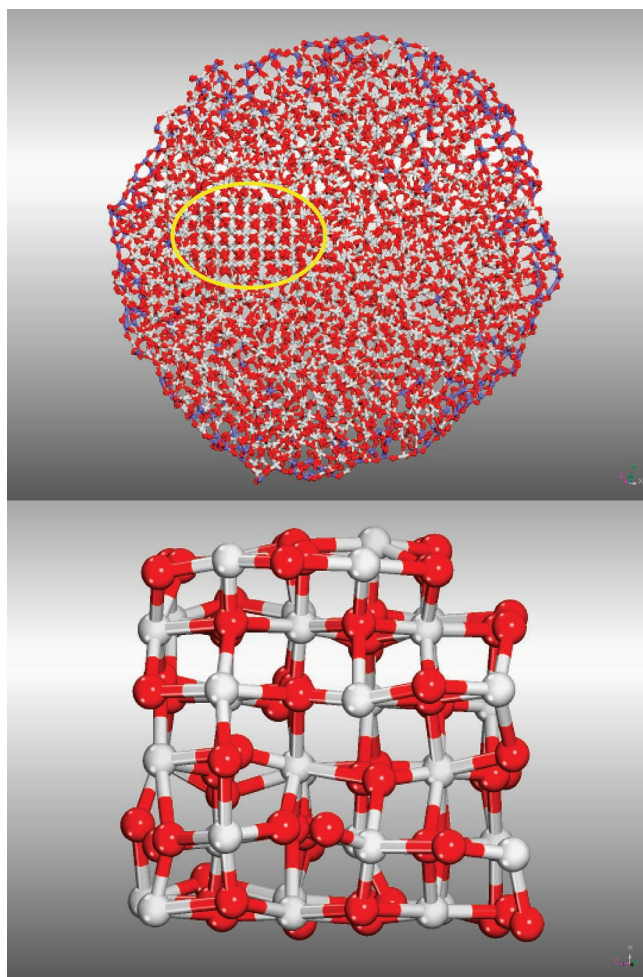


Figure 6. (Top) Atomistic structure of the Ti doped CeO₂ nanocrystal showing the embryonic stages of spontaneous nucleating seed formation, which occurs within the core region (CeO₂ rich) and away from the (TiO₂ rich) surface. (Bottom) An enlarged segment of the fluorite-structured crystalline seed. Ce is colored white, Ti, blue, and O, red. The structure was taken after 200 ps of MD simulation, which can be usefully correlated with the energy, Figure 5.

radially from the crystalline seed located at the center, is available from the Supporting Information.

During crystallization, the (amorphous) Ce, Ti, and O ions have high mobility. However, once they crystallize, mobility is lost; rather they simply vibrate about their lattice site. One can observe, from Figure 5, that the energy has converged after 500 ps, which shows that both nanoparticles are no longer crystallizing. Figure 8a shows the structure of the Ti–CeO₂ nanocrystal after 1000 ps of MD simulation (at 3750 K), and Figure 8b, the same nanocrystal 50 ps later. The bonding network between atoms is retained in Figure 8a and b thus providing an obvious graphical illustration of how far the ions have moved in 50 ps. Clearly, in the center of the nanoparticle, there is almost no mobility; rather it appears crystalline. Conversely, at the surface, one can observe significant displacements of Ti, Ce, and O. The simulations show that, at this temperature, ions comprising the outer (predominantly TiO₂) shell remain highly mobile, which is indicative of an amorphous perhaps molten phase. Therefore we suggest that the encapsulating outer shell inhibits seed formation thus preventing a viable nucleating seed from spontaneously evolving at the surface.

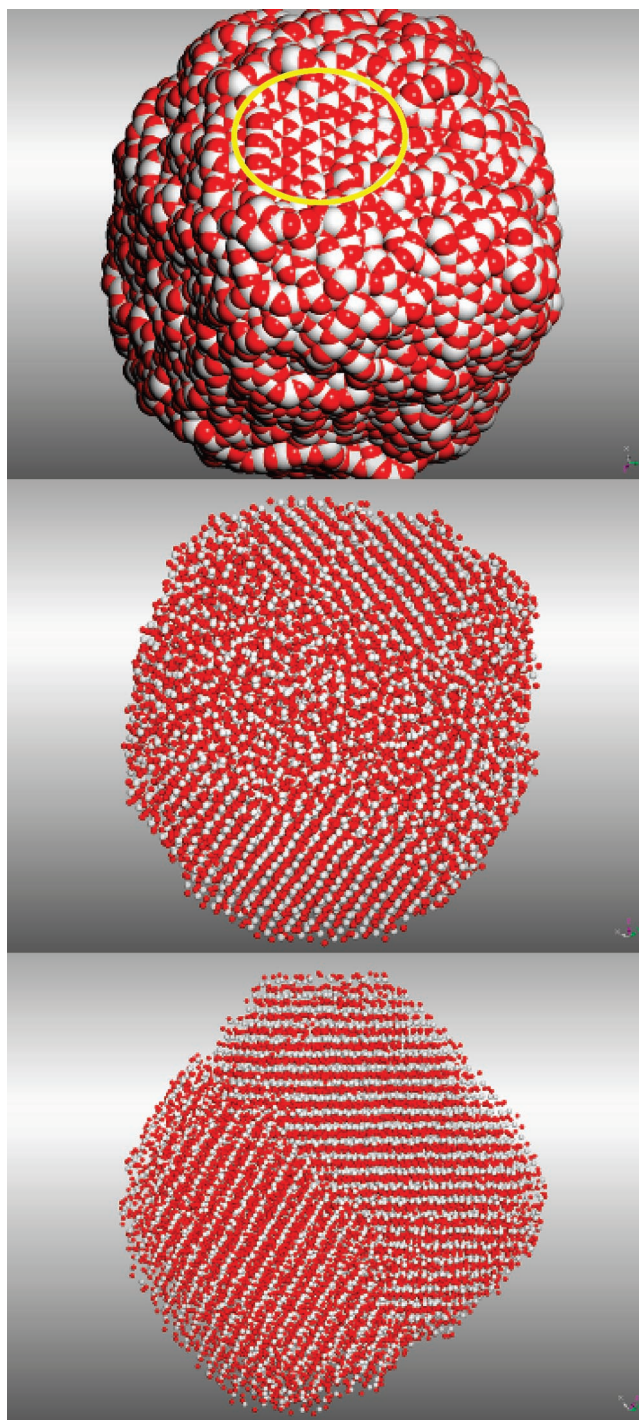


Figure 7. (Top) Atomistic structure of the undoped (pure) CeO₂ nanocrystal showing the embryonic stages of spontaneous nucleating seed formation, which evolves at the surface (yellow circle). Image taken after 150 ps; correlate with Figure 5. (Middle) Image after 325 ps of MD simulation, with smaller atom sizes to reveal that two nucleating seeds have evolved at different places at the surface. (Bottom) After 1425 ps of MD simulation. The crystallization fronts, emanating from the two seeds, have coalesced resulting in the formation of a grain boundary; note the boundary plane is curved. Ce is colored white, and O is red. The sphere sizes have been changed to allow viewing of the inner structure.

The final, low (273 K) temperature structures are shown in Figure 9. The (undoped) CeO₂ nanocrystal accommodates a polyhedral morphology with {111} and {100} facets. Conversely, the Ti-doped CeO₂ is spherical. Experimentally, CeO₂ and Ti–CeO₂ nanoparticles, Figure 10, crystallized in flame

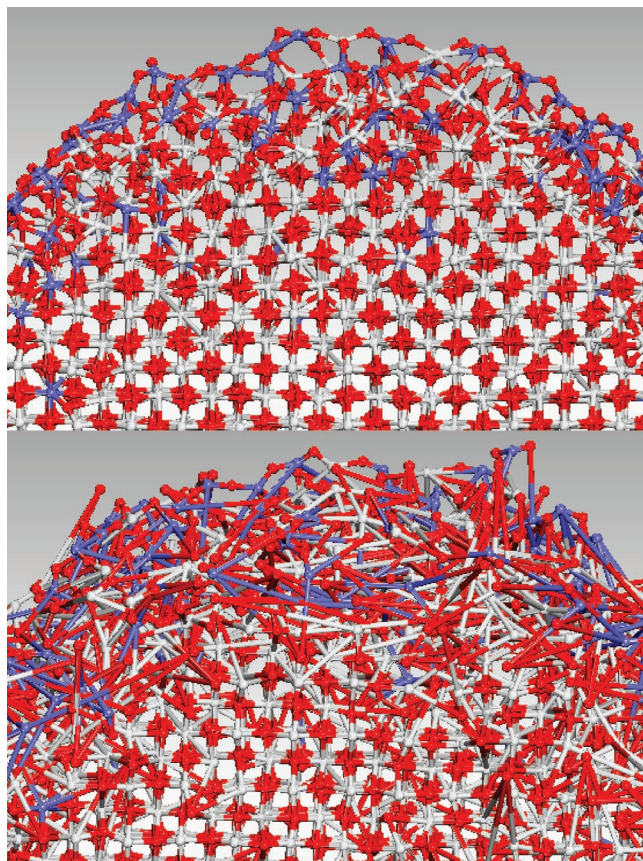


Figure 8. (Top) Ball and stick model of the Ti-doped CeO_2 nanocrystal taken after 1000 ps; crystallization had finished completely by 500 ps (Figure 5). Bottom: After 1050 ps. The bonding network has been retained to show more clearly how far the atoms move from their starting point in 50 ps. In particular, the ions comprising the inner core region (predominantly Ce, O) remain at their (crystallographic) lattice positions. Conversely, ions within the outer region (predominantly Ti, O) can be seen to have moved significantly from their starting positions indicating an amorphous/molten shell, which encapsulates an inner crystalline core. Note that Ce ions in this outer shell also exhibit high (amorphous) mobility. Ce is colored white, Ti, blue, and O, red.

exhibit polyhedral and spherical morphologies, respectively.² Figure 11 shows more clearly the low-temperature Ti– CeO_2 nanocrystal with the outer amorphous Ti(Ce) O_2 shell encapsulating an inner CeO_2 core; a high-resolution TEM image of a Ti-doped nanoparticle is also shown for comparison. We note that some Ce ions have migrated to the surface and, conversely, some Ti ions have migrated from the encapsulating shell into the core region.

Nanorods. Similar to the CeO_2 nanocrystal, crystallization in the (undoped) CeO_2 nanorod proceeded, in all cases, via the spontaneous evolution of a fluorite-structured crystalline seed exposing $\{111\}$ at the surface, and in the Ti– CeO_2 nanorods, the crystalline seeds always evolved in core regions and not at the surface.

The final, low temperature structures of the undoped and Ti-doped CeO_2 nanorods are shown in Figures 12 and 13, respectively, with side views in Figure 14. The CeO_2 nanorod exhibits $\{111\}$ and $\{100\}$ facets with a hexagonal cross section. Conversely, the Ti– CeO_2 nanorod does not exhibit any discernible facet; rather a circular cross section is observed facilitating cylindrical morphologies. Similar to the nanocrystal, the Ti– CeO_2 nanorod comprises an inner crystalline CeO_2 core, which is encapsulated by an amorphous outer shell.

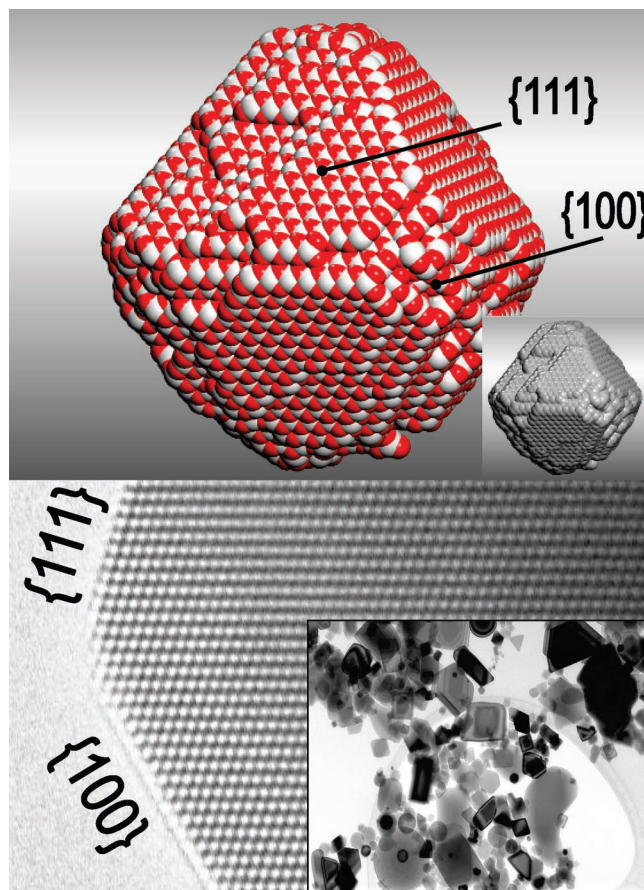


Figure 9. (Top) Graphical image of the (undoped) CeO_2 model nanocrystal; inset shows surface rendered model. Ce is white, and O, red. (Bottom) High-resolution TEM image of an (undoped) CeO_2 nanocrystal showing $\{100\}$ and $\{111\}$ type facets; inset shows a low magnification TEM image of CeO_2 nanocrystals.

Nanorods fabricated experimentally, Figure 1, proffer $\{100\}$ and $\{110\}$ surfaces.²³ Our structural models comprise $\{111\}$ and $\{100\}$, but we do not see $\{110\}$. We suggest that the discrepancy here is because our simulated crystallizations were performed in a vacuum. Conversely, experimental synthesis was achieved via a hydrothermal method.⁶ Certainly, in the future the influence of solvent can be explored; simulating the effect of a surface in water is now well established.⁹

Nanoporous Framework Architectures. The embryonic, fluoride-structured crystalline seeds that spontaneously evolve in the nanoporous CeO_2 and Ti– CeO_2 are shown in Figure 15a and b, respectively. Similar, to the nanoparticles and nanorods, viable nucleating seeds evolved at the surface (CeO_2) and within the core regions (Ti– CeO_2).

To determine whether, after crystallization, the outer shell of Ti(Ce) O_2 remained amorphous/molten within the framework Ti– CeO_2 system, the mean square displacements of the Ce, Ti, and O ions were calculated and are shown in Figure 16. The figure reveals fast ion mobility of the oxygen ions and also high mobility of the Ti ions. In a fluorite structure, cation mobility would be expected to be much smaller and therefore the figure indicates that the Ti(Ce) O_2 shell remains amorphous, even after crystallization (of the core). Ce mobility is also high, which can be attributed to Ce ions within the shell region.

(23) Zhou, K. B.; Wang, X.; Sun, X. M.; Peng, Q.; Li, Y. D. *J. Catal.* **2005**, *229*, 206–212.

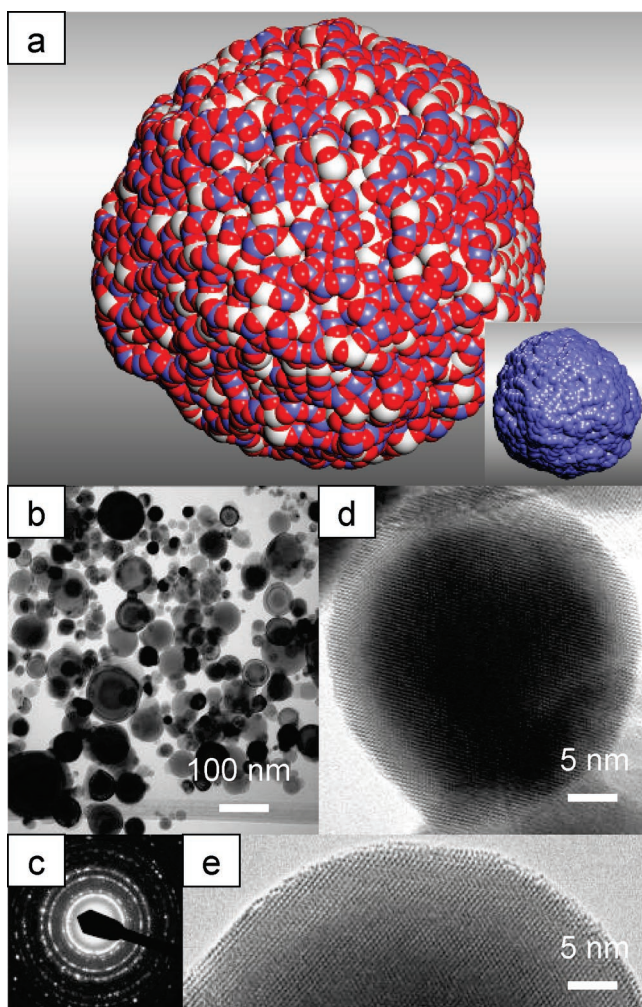


Figure 10. (a) Graphical image of the Ti-doped CeO₂ model nanocrystal. Ce is colored white, Ti, blue, and O, red. Single-crystal CeO₂ nanospheres doped with 6.25 atom % Ti: (b) Low magnification TEM; (c) diffraction pattern from many particles; (d, e) high-resolution TEM images of the nanospheres showing them to be single crystals.

The final, low temperature structures of the CeO₂ and Ti–CeO₂ framework material are shown in Figure 17. Multiple unit cells ($2 \times 5 \times 5$) of the framework CeO₂ are shown in Figure 18a to reveal more clearly the interconnecting channels. Similarly, an accessible surface model ($1 \times 3 \times 2$) of framework Ti–CeO₂ is shown, Figure 18b, to reveal more clearly the connectivity of channels along all three dimensions.

The framework structure of pure CeO₂ is faceted and expresses {111} and {100} surfaces at the pores and channels facilitating a hexagonal cross section (Supporting Information). Conversely, the pores and channels comprising Ti-doped CeO₂ are smooth and do not express any particular facet. Clearly, one cannot assign Miller indices to help describe the structure; rather we suggest that these structures are better described using minimal surfaces. For example, the framework structure shown in Figure 18b conforms closely to a (P) minimal surface.¹⁷ Experimentally, it is difficult to characterize, at the atomistic level, the cavity and interconnecting channel system,⁷ and therefore we propose that our simulations will help provide experiment with insights into possible model structures.

Microstructure. The nanocrystals, nanorods, and framework materials comprise a wealth of microstructural features. These include grain boundaries and grain junctions, dislocations, and

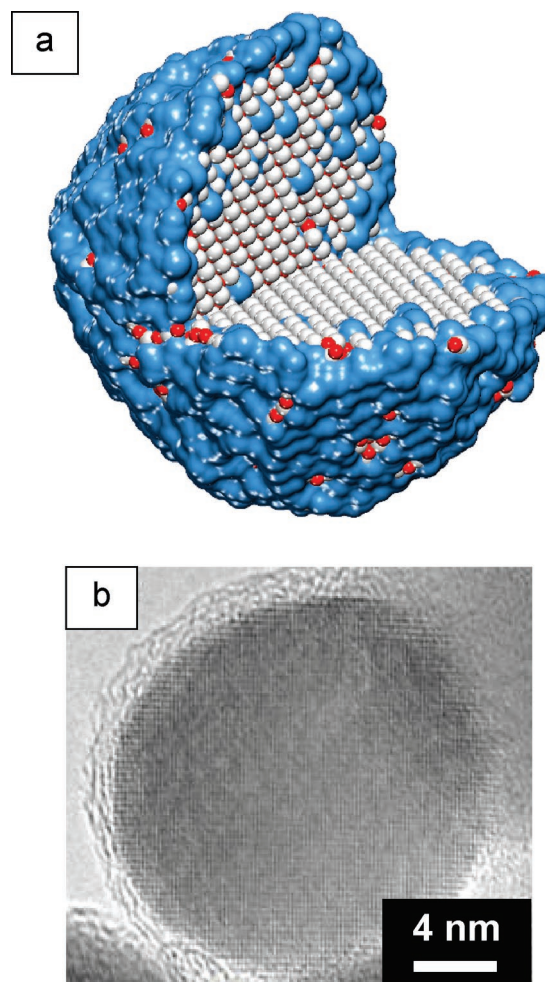


Figure 11. (a) Molecular graphics image depicting the structure of the TiO₂ shell (blue) encapsulating an inner CeO₂ core. The nanocrystal has been cut away to show, more clearly, the outer shell. Ti is blue, Ce is white, and O is red; Ti is surface rendered. (b) High-resolution TEM image of a CeO₂ nanoparticle doped with 12.5 atomic % of Ti. The image shows the TiO₂ shell encapsulating the inner CeO₂ core.

isolated and associated point defects including both anion and cation vacancies. Molecular graphic images depicting atomistic structures of a variety of microstructural features can be found in the Supporting Information.

Discussion

Experimentally, spherical, single-crystal CeO₂ nanoparticles can be synthesized when doped with titanium; undoped CeO₂ nanocrystals present polyhedral morphologies with {111} and {100} facets.² Our structural models, generated by simulating, in part, the synthesis, thus yield quantitatively accurate results. Moreover, these models evolved during the crystallization; no (artificial) adjustment in the atomistic structure is allowed during the simulation apart from those derived from modifying the simulation conditions (i.e., temperature, pressure, etc.).

Simulation is not valuable if used solely to generate models that simply compare favorably with experiment; rather they need to offer some predictive capability if they are to help support and complement experiment. Here, the simulations are able to rationalize the evolution of spherical (Ti–CeO₂) and polyhedral (pure CeO₂) morphologies by helping experiment unravel the mechanisms pertaining to the crystallization. In particular, if

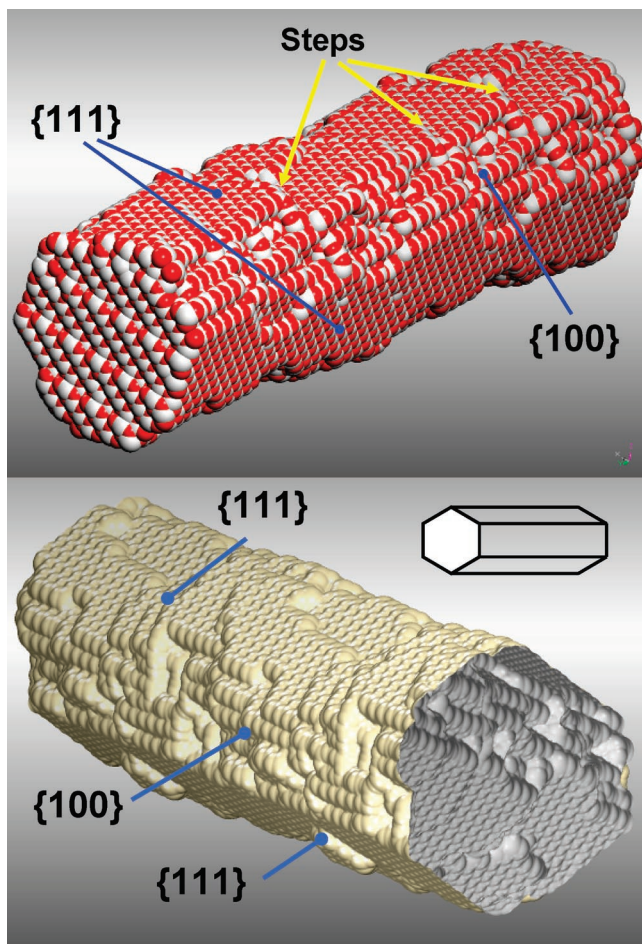


Figure 12. Final, low temperature images of the undoped CeO_2 nanorod. (Top) Atomistic sphere model showing the $\{111\}$ with steps and $\{100\}$ facets. Bottom, surface rendered model. Ce is white, and O, red.

we look closely at the simulation (and in particular, the molecular graphics animation of the crystallization), the dopant Ti ions form a $\text{Ti}(\text{Ce})\text{O}_2$ shell (predominantly TiO_2 although some Ce remains at the surface region) around the inner CeO_2 core region. This shell inhibits the spontaneous evolution of embryonic $\text{CeO}_2\{111\}$ facets on the *surface* of the $\text{Ti}-\text{CeO}_2$ nanoparticle because it remains in an amorphous/molten state (Figure 8). Accordingly, the only place a viable (nucleating) seed can spontaneously evolve is in the (CeO_2) core region of the $\text{Ti}-\text{CeO}_2$ nanoparticle. As this seed grows, emanating radially from the seed, it is encapsulated by an amorphous/molten shell, and therefore there is no energetic driving force to expose low-energy (i.e., $\{111\}$) facets; rather the shell, because it is molten/amorphous, accommodates a spherical morphology to minimize its surface energy. After the CeO_2 has crystallized completely, the outer TiO_2 remains amorphous/molten (Figure 7) and retains this configuration after cooling to low temperature. We suggest the amorphicity of the outer shell is compounded by the lattice misfit between CeO_2 and TiO_2 .

Experimentally, we synthesized $\text{Ti}-\text{CeO}_2$ nanocrystals by spraying a fine mist of solutions containing the cerium and titanium precursors, dissolved in alcohol.² The mist was ignited directly by pilot torches in the line of the spray, leading to instantaneous combustion of the metal precursors to form metal oxides CeO_2 and $\text{Ti}-\text{CeO}_2$. The products (nanoparticulate

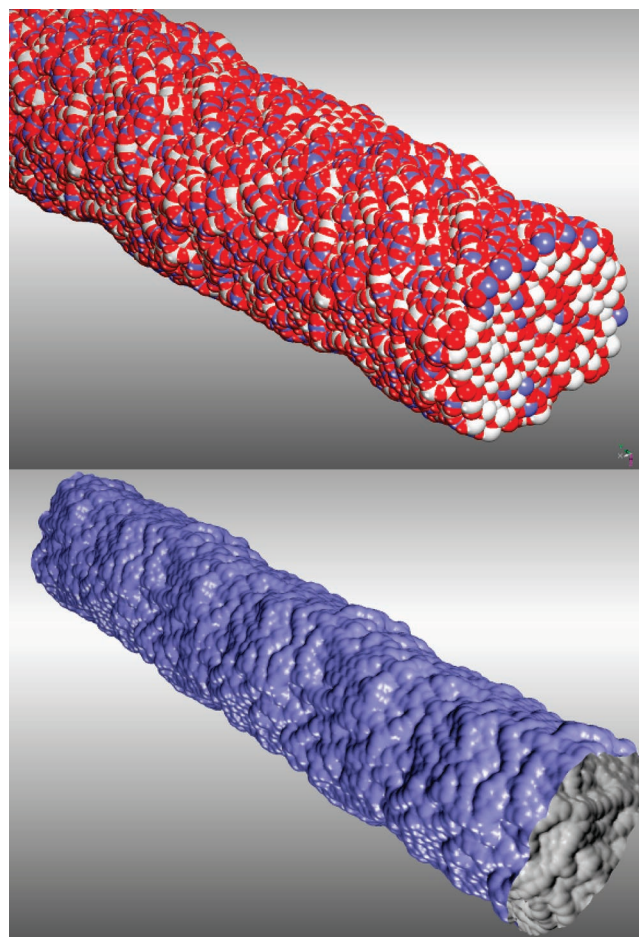


Figure 13. Final, low temperature images of the Ti-doped CeO_2 nanorod. (Top) Atomistic sphere model. (Bottom) Surface rendered model. No facets are evident; rather the nanorod exhibits a cylindrical shape.

smoke) were rapidly quenched downstream from the combustion zone facilitating control over the crystallization of the nanoparticles. Coupled with the results of our simulations, we propose a mechanism for facilitating spherical nanocrystals. In particular, as the nanoparticles cooled, when moving away from the flame, the inner CeO_2 core crystallized before the outer TiO_2 shell. Specifically, the temperature was sufficient to facilitate complete crystallization of CeO_2 , while retaining the TiO_2 shell in an amorphous/molten state, which inhibited the spontaneous evolution of a nucleating seed at the surface.

Inspection of nanorods and nanoporous $\text{Ti}-\text{CeO}_2$ reveals analogous behavior. Specifically, $\text{Ti}-\text{CeO}_2$ nanotubes become cylindrical, and the nanoporous $\text{Ti}-\text{CeO}_2$ exhibit a minimal surface¹⁷ with no discernible facets.

As far as we are aware there are no reported structures for Ti-doped CeO_2 nanorods and nanoporous architectures, and therefore we predict that the nanorod will be cylindrical and the nanoporous material will exhibit an architecture conforming to a (P) minimal surface;¹⁷ we await their synthesis.

This study provides a platform on which one can build to simulate other synthetic methods. We envisage rather simple additions of gas atoms to convey hydrostatic pressure on the system. “In solution” simulations are also possible.^{8,9}

Framework ceria nanostructures have been synthesized by various groups (for example see refs 3, 7) with structures similar to our atomistic models. Central to the reactivity of nanoporous

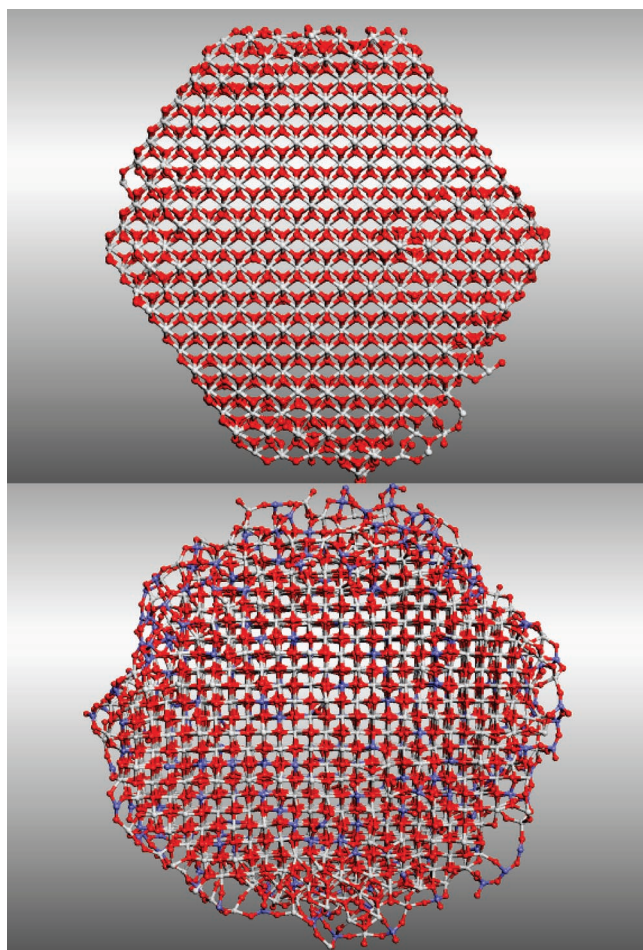


Figure 14. Side profiles of the nanorods shown in Figures 12 and 13, respectively. (Top) Undoped CeO₂. (Bottom) Ti-doped CeO₂ nanorods. Ce is white, Ti, blue, and O, red.

framework CeO₂ are the surfaces exposed by the internal pore and channel network, which are difficult to characterize experimentally. Accordingly, our simulations offer the prediction that {111} and {100} surfaces are proffered. We note also that, similar to our models, Deshpande points to "complete accessibility of the mesopores".⁷

Conclusion

Contemporary materials are demonstrating increasing structural complexity that is seriously challenging the ability of "the simulator" to generate atomistic models, which are sufficiently realistic in that they can usefully describe their structure and predict their properties. Ultimately, complexity evolves from synthesis, and therefore to capture such complexity within an atomistic model, we have attempted to simulate synthesis.

In particular, we have "simulated synthesis" to generate full atomistic models of ceria nanocrystals, nanorods, and nanoporous framework architectures. We capture the important features of (experimental) synthesis in two respects: First, the formation of amorphous nanoparticles and their self-assembly into nanorods and nanoporous architectures, and second, the crystallization from the amorphous oxide precursors. The final atomistic models show quantitative agreement with experiment. Specifically, ceria nanocrystals, fabricated (experiment) by crystallization in flame, comprise polyhedral nanocrystals with {111} and {100} facets. However, when doped with Ti, the nanoc-

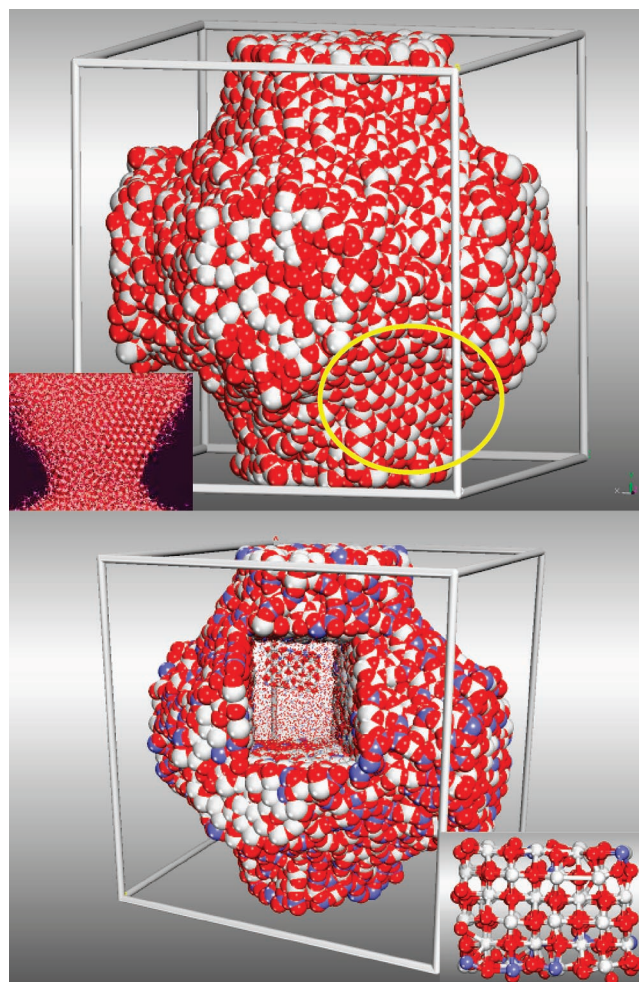


Figure 15. Spontaneous evolution of the nucleating seed in the nanoporous framework structures. (Top) Pure CeO₂. Here the seed evolves at the surface (yellow oval). Inset shows more clearly the partially crystalline framework. (Bottom) Ti–CeO₂. Here, the seed evolves in the core region of which a part is represented by very small spheres to reveal the crystalline seed within. Inset shows the crystalline seed enlarged. The sphere sizes have been changed to allow viewing of the inner structure.

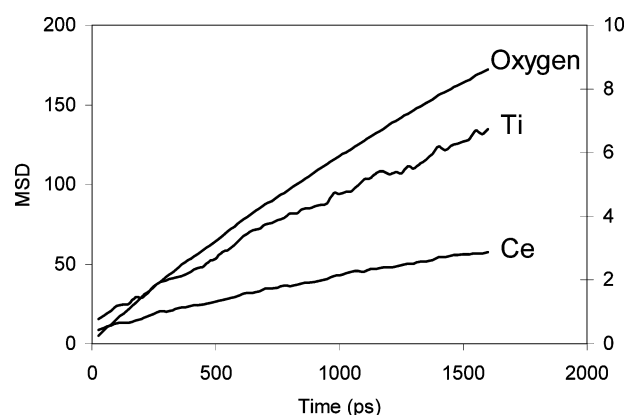


Figure 16. Mean square displacements (MSD) of the ions (Å²) at 2600 K, calculated as a function of time, for the nanoporous Ti–CeO₂ framework. Primary ordinate (left) is Oxygen MSD and secondary ordinate, right, corresponds to Ti and Ce MSD.

ystals become spherical. Our models of pure ceria nanocrystals exhibit {111}, {100} terminated polyhedra, and Ti-doped CeO₂ nanocrystals are spherical in quantitative agreement with experiment.

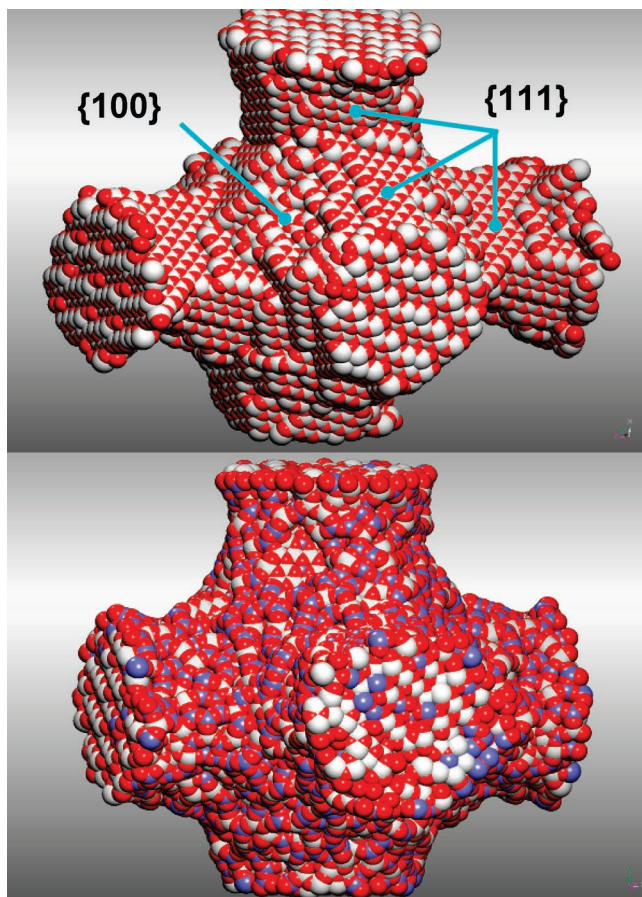


Figure 17. Final, low temperature nanoporous framework architectures. (Top) CeO₂. (Bottom) Ti–CeO₂. Slightly more than the primitive unit cells are shown. Ce is colored white, Ti, blue, and O, red.

Simulations, and the models they facilitate, are of little value unless used to help or advance experiment. Here, we have rationalized, in partnership with experiment, the formation of spherical nanocrystals. Specifically, animations depicting the crystallization of undoped CeO₂ reveal nucleating seeds, which spontaneously evolve at the *surface* of the nanoparticle and present stable {111} facets, thus facilitating polyhedral morphologies. Conversely, when doped with Ti, the Ti ions locate preferentially at the surface of the nanoparticle forming a (predominantly) TiO₂ outer shell which encapsulates the inner (predominantly) CeO₂ core. This shell suppresses the evolution of nucleating seeds at the surface, and therefore as the nanoparticle cools, crystallization is forced to proceed via the evolution of a nucleating seed in the CeO₂ core region. Moreover, as crystallization progresses, emanating radially from the nucleating seed, it is encapsulated by the TiO₂ shell, which accommodates a spherical morphology to minimize the surface energy. As the crystallization front encroaches into the TiO₂ shell, it does not facilitate crystallization of the TiO₂, which remains amorphous even at low temperature compounded, in addition, by the lattice misfit between the CeO₂ core and TiO₂ shell. Ti–CeO₂ nanocrystals synthesized in this manner are therefore spherical. Our results have wider implications in that we have rationalized a strategy for generating spherical nanocrystals in general. In particular, we *predict* that spherical inorganic nanocrystals can be synthesized via crystallization if one forces the nucleating seed to evolve in the core region

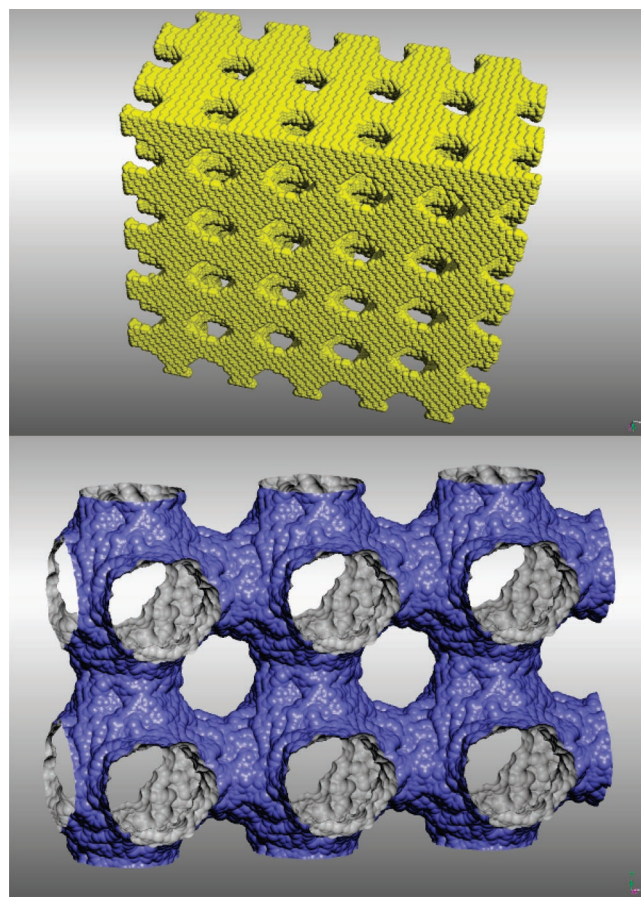


Figure 18. Final, low temperature nanoporous framework architectures. (Top) CeO₂ sphere model, approximately $2 \times 5 \times 5$ simulation cells, with only Ce atoms, colored yellow, shown. (Bottom) Ti–CeO₂ surface rendered model; approximately $1 \times 2 \times 3$ simulation cells.

rather than at the surface. This may be facilitated by doping the outside with a material of lower melting point, and as the nanocrystal cools, it will crystallize from the inside and/or extrinsically dope with ions that disrupt the evolution of nucleating seeds (particularly the surface facet) on the outside of the nanoparticle.

These results have important implications for industry. Specifically, ceria nanoparticles are one of the key abrasive materials for chemical–mechanical planarization of advanced integrated circuits.² However, because (undoped) CeO₂ nanocrystals are polyhedral, they scratch the silicon wafers and increase defect concentrations. Conversely, when doped with Ti, the nanocrystals are rendered spherical, and similar to “tiny ball-bearings”, they polish the surface without scratching it; polishing defects are reduced by 80% and silica removal rates are increased by 50%, facilitating precise and reliable mass-manufacturing of chips for nanoelectronics. In particular, nanoabrasives commanded 60% of the \$1 billion market in nanomaterials in 2005.²

Similar to zeolitic chemistry and classification, spherical nanocrystals may be envisaged to constitute “Secondary Building Units” to construct a broad range of architectures. Here, we have used them to generate nanorods and nanoporous framework materials. In addition, for nanorods and nanoporous ceria we predict that the addition of Ti to the surfaces facilitates the removal of faceting at the surfaces thus rendering them

smooth, similar to a minimal surface. Such structures are likely to demonstrate surface reactivities in marked contrast from the undoped parent material.

At present our simulations provide a "rough sketch" of experimental synthesis; nevertheless we have shown them to be quantitatively reliable and predictive. Moreover, our approach can be used as a platform to build upon and design new simulations that better capture the nuances and subtleties of synthesis that are ultimately responsible for introducing structural complexity.

Acknowledgment. Prof. Jacek Klinowski (Cambridge, U.K.) for invaluable discussions of minimal surfaces. Cambridge-Cranfield HPCF, EPSRC (GR/S48431/1, GR/S48448/01, and GR/S84415/01).

Supporting Information Available: Movie depicting the crystallization of the Ti–CeO₂ nanocrystal; molecular graphics images of nanoporous CeO₂ and Ti–CeO₂ showing the pore and channel structure and microstructural features including surfaces, grain boundaries, and grain junctions.

JA070893W